J. Astrophys. Astr. (December 2017) 38:71
https://doi.org/10.1007/s12036-017-9482-5

Relativistic Dynamics in a Matter-Dominated Friedmann Universe

M. LANGA, D. S. WAMALWA* and C. MITO

Astronomy and Astrophysics Group, Department of Physics, University of Nairobi, P. O. Box 30197-00100, Nairobi, Kenya.
*Corresponding author. E-mail: dismasw@yahoo.com

MS received 19 June 2017; accepted 2 August 2017; published online 27 November 2017

Abstract. The energy density of the universe is estimated to be composed of 68% dark energy. Dark energy is associated with the accelerated expansion of the universe. In this work, we consider the evolution of the number density $n(z)$ and light intensity $I(z)$ of galaxies with redshift z for a matter-dominated Friedmann universe in the presence of dark energy and compare the results with a matter-dominated Friedmann universe without dark energy effects. Computational results of $n(z)$ and $I(z)$ are presented in a suitable form for comparison with future observed dependencies to test the fractal-homogeneous models of open, closed and flat matter-dominated universe. From our results, there was increased structure formation in the universe from $z = 0$ to $z \approx 1$ when the rate of growth started to slow down. Furthermore, there is reduced structure formation for a universe driven by dark energy as compared to one without dark energy.

Keywords. Dark energy—redshift—number density—light intensity—Friedmann—fractal

1. Introduction

The cornerstone of the standard theory of cosmology is the Lambda Cold Dark Matter (ΛCDM) model. This model embraces the cosmological principle, i.e., the universe is homogeneous and isotropic on large scales. The homogeneity and isotropy properties imply that our universe is translationally and rotationally invariant. The cosmological principle does not follow from the laws of physics but rather seems to compliment them and has, therefore, received criticism (Michal 1989). However, the homogeneity and isotropy assumptions make it possible to describe the universe by the Friedmann-Lemaitre-Robertson-Walker (FLRW) metric. As much as there are many structure formation theories of the universe, the ΛCDM is the most consistent and widely accepted theory of structure formation in the universe. This model has been supported by isotropy of the radio sources, isotropy of the cosmic microwave background and isotropy of the x-ray background (Borgani 1995). Furthermore, the Sloan Digital Sky Survey (SDSS) data analysis (Sarkar & Pandey 2016) showed that the small inhomogeneities of the galaxy distribution at small length scales tilt towards homogenization at large scales (>50 Mpc). In spite of the success of the ΛCDM model, the tridimensional redshift galaxy surveys cast doubt on the validity of the model and the cosmological principle in general. As a result, we have a camp of physicists who believe that our universe is not only inhomogeneous on small length scales (<10 Mpc) but the inhomogeneities extend up to the present large scale observational limits (>100 Mpc) without any clear tendency to homogenization (Labini & Pietronero 1996; Park *et al.* 2016 at arXiv:1611.02139). It is believed that these inhomogeneities depict fractality of the universe, i.e., a universe in which structures at small scales appear similar to those at large scales (Labini & Pietronero 1996). Fractal models are characterized by dimension two ($D_F = 2$) while homogeneous models by dimension three ($D_F = 3$). Fractal scale is an implicit representation of information, content and its value is a geometric significance of the area. Current studies show that our universe is a complex hologram (Mureika 2007). Fractal holography is a pointer to fractal universe. If the fractal model is indeed true, then consideration of small scale homogeneities as small density perturbations as used in ΛCDM is not true.

In General Relativity (GR), quantities like correlation functions, power spectrum and hubble parameters that are based on homogeneity assumption would also not be true. Furthermore, such correlation functions cannot be defined as samples that do not show any clear tendency to homogenization and have no defined mean density to interpret the statistical data. Moreover, the inhomogeneity of the universe would affect distance measurements as it would affect travel of light rays and calibration of clocks and rods for observers. Thus, the fractal debate compels us to solidly establish as to whether or not our universe is indeed Friedmann on large scales. However, to do this, one needs huge and reliable astronomical data that is beyond our current technology. Even the largest SDSS data covers only a quarter of the sky (Kazuhiro 2003; Joyce *et al.* 2005). In this work, we adopt the view that the Friedmann model is correct by considering three astronomical quantities with an underlying Friedmann metric. We assume that we are given huge astronomical data for measured redshift z, number density of galaxies per solid angle in a given direction $n(z)$ and light intensity $I(z)$. We establish the connection between these quantities using Einstein field equations. In an earlier work (Wamalwa 2016), this problem was highlighted for a matter-dominated Friedmann universe while ignoring the effects of dark energy. Pertinent to this paper is establishing the relationship between the quantities for Friedmann matter dominated universe in the presence of dark energy effects. In GR, all forms of energy gravitate so that ground state energy (vacuum energy) should impact the dynamics of expansion of the universe. This energy has experimentally been found to be linked to Einstein's cosmological constant (Filippenko 1998). Therefore, we consider Einstein's equations with a cosmological constant in describing dynamics and evolution of the universe. We shall prepare the analytical results in suitable MATLAB plots for comparison with future observed dependencies. From the results, it is possible to judge from any given experimental curve for which the above quantities have been measured if the universe is flat, closed or open and as to whether or not the Friedmann model should be dropped in favour of fractal model.

The paper is organized as follows: In section 2, we consider Einstein field equations with cosmological constant for a matter-dominated Friedmann universe while in section 3 and section 4, we establish how light intensity and number density vary with redshift respectively. In section 5, we make matlab plots of light intensity vs. redshift and number density vs. redshift and discuss our results before making conclusions in section 6.

2. Einstein field equations based on Friedmann metric

Consider the second rank covariant metric tensor

$$g_{\mu\nu} = \begin{pmatrix} c^2 & 0 & 0 & 0 \\ 0 & \frac{-R(t)^2}{(1+\kappa r^2)^2} & 0 & 0 \\ 0 & 0 & \frac{-R(t)^2}{(1+\kappa r^2)^2} & 0 \\ 0 & 0 & 0 & \frac{-R(t)^2}{(1+\kappa r^2)^2} \end{pmatrix},$$

so that the FLRW metric in rectangular coordinates reads

$$g = c^2 \mathrm{d}t^2 - \frac{R(t)^2}{(1+\kappa r^2)^2}(\mathrm{d}x^2 + \mathrm{d}y^2 + \mathrm{d}z^2). \tag{1}$$

Straightforward calculations based on this metric yield the components of the Ricci tensor as

$$R_0^0 = -\frac{3R''(t)}{c^2 R(t)}, \tag{2}$$

$$R^{00} = -\frac{3R''(t)}{c^4 R(t)}, \tag{3}$$

$$R_1^1 = \frac{R(t)R''(t) + 2R'(t)^2 + 8\kappa c^2}{c^2 R(t)^2} = R_2^2 = R_3^3, \tag{4}$$

$$R^{11} = \frac{8\kappa c^2 + R(t)R''(t) + 2R'(t)^2}{c^2 R(t)^4}(1+\kappa r^2)^2 = R^{22} = R^{33}, \tag{5}$$

so that we can now express the curvature scalar as

$$R = R_u^u = -\frac{3(8\kappa c^2 + 2R(t)R''(t) + 2R'(t)^2)}{c^2 R(t)^2}. \tag{6}$$

To describe the dynamics and evolution of the universe while considering the effects of dark energy, we consider Einstein field equations with cosmological constant

$$R^{\mu\nu} - \frac{1}{2}Rg^{\mu\nu} + \lambda g^{\mu\nu} = \beta T^{\mu\nu}, \tag{7}$$

where $\beta = \frac{8\pi G}{c^4}$, G is the gravitational constant, λ is the cosmological constant, $g^{\mu\nu}$ is the metric tensor, $R^{\mu\nu}$ is the Ricci tensor, R is Ricci scalar, $T^{\mu\nu}$ is the stress-energy tensor of the matter content in the universe and c is the speed of light. This matter content in the universe must be uniformly distributed if the universe is homogeneous. Furthermore, the matter content must be at rest w.r.t the coordinates otherwise direction of velocity would break isotropy of the universe. As mentioned earlier, the cosmological constant is associated with ground state vacuum energy which drives dynamics and evolution of the universe. The stress-energy tensor has the

components (Wamalwa 2016)

$$T^{00} = \rho(t) \tag{8}$$

and

$$T^{11} = T^{22} = T^{33} = \frac{(1+\kappa r^2)^2}{R(t)^2} P(t), \tag{9}$$

representing the energy and current densities respectively. $T^{\mu 0}, \mu = 1, 2, 3$ are momenta densities while $\rho(t)$ and $P(t)$ are mass density and pressure of the universe respectively. The stress energy tensor is related to Einstein tensor by the Einstein equation

$$G^{\mu\nu} = R^{\mu\nu} - \frac{1}{2} R g^{\mu\nu}. \tag{10}$$

Application of equation (10) in equation (7) yields

$$G^{\mu\nu} = R^{\mu\nu} - \frac{1}{2} R g^{\mu\nu} = BT^{\mu\nu} - \lambda g^{\mu\nu}. \tag{11}$$

For $\mu = \nu = 0$, equation (11) becomes

$$G^{00} = R^{00} - \frac{1}{2} R g^{00} = \beta T^{00} - \lambda g^{00}. \tag{12}$$

Substituting equations (3), (6), (8) into equation (12) and noting that $g^{00} = c^{-2}$ yields

$$12\kappa c^2 + 3R'(t)^2 = \beta c^4 R(t)^2 \rho(t) - \lambda c^2 R(t)^2. \tag{13}$$

Similarly, for $\mu = \nu = 1, 2, 3$, it can be shown with the aid of equations (5), (6), (9) and (11) that

$$4\kappa c^2 + 2R(t)R''(t) + R'(t)^2 = -\beta c^2 R(t)^2 P(t) - \lambda c^2 R(t)^2. \tag{14}$$

Equations (13) and (14) form our main equations for describing the dynamics and evolution of the universe. They are more general than field equations obtained earlier while ignoring the effects of dark energy (Wamalwa 2016). Clearly, these equations reduce to familiar equations without dark energy effects when we let $\lambda = 0$. We now proceed to obtain a conservation law based on these equations

2.1 *Matter-dominated Friedmann universe*

Straightforward calculation based on our field equations (13) and (14) yields

$$\frac{\mathrm{d}}{\mathrm{d}t}(c^2 \rho(t) R(t)^3) = -P(t) \frac{\mathrm{d}}{\mathrm{d}t} R(t)^3. \tag{15}$$

This means that the rate of change of the volume in the universe multiplied by negative pressure equals the rate of change of energy in the universe. If we now consider a pressureless matter-dominated universe so that $P(t) = 0$, equation (15) becomes

$$\frac{\mathrm{d}}{\mathrm{d}t}(c^2 \rho(t) R(t)^3) = 0$$

or

$$\rho(t) R(t)^3 = \alpha, \tag{16}$$

where α is a constant. This shows that the total matter content in the universe remains constant at any given time and therefore, equation (16) describes a matter-dominated Friedmann universe.

Equations (13) and (16) combine as

$$12\kappa c^2 + 3R'(t)^2 = \frac{\beta c^4 \alpha}{R(t)} - \frac{\lambda \alpha c^2}{R(t)\rho(t)}$$

so that

$$\mathrm{d}t = \frac{\mathrm{d}R}{\sqrt{\frac{\beta c^4 \alpha}{3R(t)} - \frac{\lambda \alpha c^2}{3R(t)\rho(t)} - 4\kappa c^2}}. \tag{17}$$

Equation (17) has an additional term $(\lambda \alpha c^2 / 3R(t)\rho(t))$ carrying the effect of dark energy which is usually absent in Einstein field equations without the cosmological constant.

3. Light intensity-redshift relation

Suppose at time of emission $t = t_\mathrm{e}$, light from an astronomical object starts at $r(t_\mathrm{e})$ and travels towards the origin such that at observational time $t = t_\mathrm{o}$, it reaches the origin $(r(t_\mathrm{o}) = 0)$. The Friedmann metric (see equation (1)), can be rewritten for null geodesics as

$$0 = c^2 \mathrm{d}t^2 - \frac{R(t)^2}{(1+\kappa r^2)^2} \mathrm{d}r^2$$

or

$$c\dot{t} = \pm \frac{R(t)\dot{r}}{1+\kappa r^2}. \tag{18}$$

Using the assumption that $\dot{t}$ is positive while $\dot{r}$ is negative, this equation can be written as

$$\frac{c}{R(t)} \mathrm{d}t = -\frac{1}{1+\kappa r^2} \mathrm{d}r. \tag{19}$$

Performing integration of equation (19) over $(t_\mathrm{e}, t_\mathrm{o})$ and $(r(t_\mathrm{e}), r(t_\mathrm{o}))$, we get

$$\int_{R(t_\mathrm{e})}^{R(t_\mathrm{o})} \frac{\mathrm{d}R}{\sqrt{R(t)}\sqrt{\frac{\beta c^2 \alpha}{3} - \frac{\lambda \alpha}{3\rho(t)} - 4\kappa R}} = -\int_{r(t_\mathrm{e})}^{r(t_\mathrm{o})} \frac{1}{1+\kappa r^2} \mathrm{d}r. \tag{20}$$

This equation is more general and suitable for describing dynamics as it contains an extra cosmological term on its left-hand side earlier present in equation (17). We can solve equation (20) for three different cases of κ, i.e., $\kappa = -1$ (open universe), $\kappa = 0$ (flat universe) and $\kappa = 1$ (closed universe). Straightforward calculations based on equation (20) yield

$$r(z) = \begin{cases} \sqrt{\frac{12\rho(t_o)R(t_o)}{\beta c^2\alpha\rho(t_o)-\lambda\alpha}} - \sqrt{\frac{12\rho(t_o)R(t_o)}{(\beta c^2\alpha\rho(t_o)-\lambda\alpha)(1+z)}}, & \kappa = 0 \\ \frac{\sqrt{12\rho(t_o)R(t_o)}\left[\sqrt{(\beta c^2\alpha\rho(t_o)-\lambda\alpha)(1+z)-12\rho(t_o)R(t_o)}-\sqrt{\beta c^2\alpha\rho(t_o)-\lambda\alpha-12\rho(t_o)R(t_o)}\right]}{\sqrt{\beta c^2\alpha\rho(t_o)-\lambda\alpha-12\rho(t_o)R(t_o)}\sqrt{(\beta c^2\alpha\rho(t_o)-\lambda\alpha)(1+z)-12\rho(t_o)R(t_o)}+12\rho(t_o)R(t_o)}, & \kappa = 1 \\ \frac{\sqrt{12\rho(t_o)R(t_o)}\left[\sqrt{(\beta c^2\alpha\rho(t_o)-\lambda\alpha)(1+z)+12\rho(t_o)R(t_o)}-\sqrt{\beta c^2\alpha\rho(t_o)-\lambda\alpha+12\rho(t_o)R(t_o)}\right]}{\sqrt{\beta c^2\alpha\rho(t_o)-\lambda\alpha+12\rho(t_o)R(t_o)}\sqrt{(\beta c^2\alpha\rho(t_o)-\lambda\alpha)(1+z)+12\rho(t_o)R(t_o)}+12\rho(t_o)R(t_o)}, & \kappa = -1, \end{cases} \tag{21}$$

where we have used the relations: $r(t_e) = r(z)$ since t_e is a function of z; $R(t_e) = R(t_o)/(1+z)$ and $\rho(t) = \rho(t_o)$ is the density of the universe at observational time, t_o. All the three cases in equation (21) can be written as

$$r(z) = \frac{\sqrt{12\rho(t_o)R(t_o)}\left[\sqrt{\left(\beta c^2\alpha\rho(t_o)-\lambda\alpha\right)(1+z)-12\kappa\rho(t_o)R(t_o)}-\sqrt{\beta c^2\alpha\rho(t_o)-\lambda\alpha-12\rho(t_o)\kappa R(t_o)}\right]}{\sqrt{\beta c^2\alpha\rho(t_o)-\lambda\alpha-12\kappa\rho(t_o)R(t_o)}\sqrt{\left(\beta c^2\alpha\rho(t_o)-\lambda\alpha\right)(1+z)-12\rho(t_o)\kappa R(t_o)}+12\rho(t_o)\kappa R(t_o)}, \tag{22}$$

where $\kappa = -1, 0, 1$. If we define

$$\begin{aligned} a_1 &= \beta c^2\alpha\rho(t) - \lambda\alpha - 12\kappa\rho(t_o)R(t_o), \\ a_2 &= (\beta c^2\alpha\rho(t_o) - \lambda\alpha)(1+z) - 12\kappa\rho(t_o)R(t_o), \end{aligned} \tag{23}$$

then, equation (22) becomes

$$r(z) = \frac{\sqrt{12\rho(t_o)R(t_o)}(\sqrt{a_2}-\sqrt{a_1})}{\sqrt{a_1a_2}+12\kappa\rho(t_o)R(t_o)}. \tag{24}$$

Suppose our astronomical object e.g. star or galaxy located at $r = 0$ is emitting light at an absolute power L. In some time interval, we consider the light emitted dt_e. At an observation time t_o, an observer measures the brightness I of that light which he receives at a redshift z. The observer's position of reception of this light is given by equation (22). As photons pass through space, they get redshifted. This means that the energy that passes through the sphere of radius, $r = r(z)$ during some time interval dt_e, is the same as $1/(1+z)$. With this, we can express light intensity I, dependent on luminosity L, of luminous matter in the universe as

$$I = \frac{L\,dt_e}{(1+z)S_{r(z)}}, \tag{25}$$

where $S_{r(z)}$ denotes the surface area of the sphere of radius $r = r(z)$ at time $t = t_o$. From equation (18), we can perform integration from t_e to t_o and from the coordinates radius $r = 0$ to $r = r(z)$ to give us

$$\int_{t_e}^{t_o} \frac{c}{R(t)}dt = \int_0^{r(z)} \frac{1}{1+\kappa r^2}dr. \tag{26}$$

In terms of time intervals, we can write this equation as

$$\int_{t_e+dt_e}^{t_o+dt_o} \frac{c}{R(t)}dt = \int_0^{r(z)} \frac{1}{1+\kappa r^2}dr. \tag{27}$$

Applying the fundamental theorem of integral calculus and using the relation $dt_e/dt_o = R(t_e)/R(t_o) = 1/(1+z)$, we obtain

$$I = \frac{L\left[1+\kappa\left(\frac{\sqrt{12\rho(t_o)R(t_o)}(\sqrt{a_2}-\sqrt{a_1})}{\sqrt{a_1a_2}+12\kappa\rho(t_o)R(t_o)}\right)^2\right]^2}{4\pi(1+z)^2\left(\frac{\sqrt{12\rho(t_o)R(t_o)}(\sqrt{a_2}-\sqrt{a_1})}{\sqrt{a_1a_2}+12\kappa\rho(t_o)R(t_o)}\right)^2 R(t_o)^2}, \tag{28}$$

where $S_{r(z)} = \frac{4\pi r(z)^2R(t_o)^2}{(1+\kappa r(z)^2)^2}$.

4. Number density-redshift relation

Suppose our astronomical objects (e.g. supernovae or galaxies) under consideration are uniformly distributed in the universe so that we count how many galaxies we see in a given redshift interval. If N is the number of galaxies per unit volume of the space with metric $(dr^2 + r^2d\theta^2 + r^2\sin^2\theta d\theta)/(1+\kappa r^2)^2$, and $r^2\sin\theta d\theta d\varphi dr/(1+\kappa r^2)^3$ is the volume element, then the number of galaxies between r and dr is

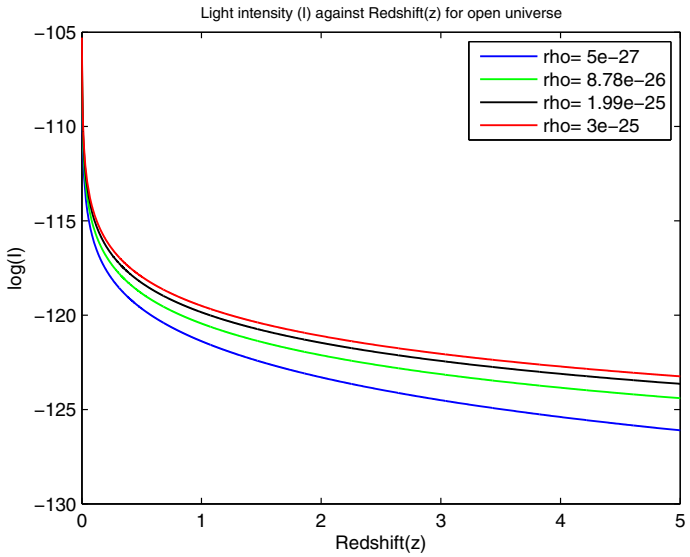

Figure 1. Plot of $\log(I)$ against z for $0 \leq z \leq 5$ and $\kappa = -1$ without cosmological constant (λ).

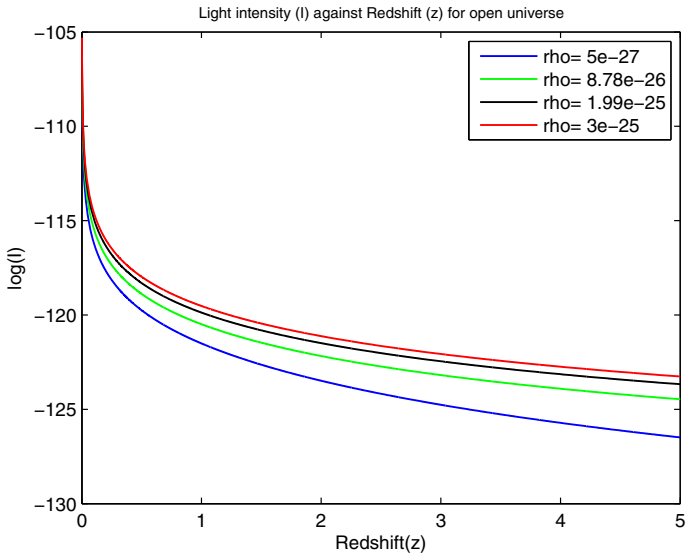

Figure 2. Plot of $\log(I)$ against z for $0 \leq z \leq 5$ and $\kappa = -1$ with cosmological constant (λ).

$4\pi r^2 \mathrm{d}r/(1+\kappa r^2)^3 N$. Therefore, the number of galaxies between coordinate hyperspheres $r(z)$ and $r(z+\mathrm{d}z)$ is given by

$$n(z)\mathrm{d}z = 4\pi r(z)^2 (1+\kappa r(z)^2)^3 N r'(z)\mathrm{d}z, \tag{29}$$

where $r'(z) = \mathrm{d}r/\mathrm{d}z$ is obtained by differentiating equation (24) as

$$\frac{\mathrm{d}r}{\mathrm{d}z} = \frac{(\beta c^2 \alpha \rho(t_\mathrm{o}))^2 \sqrt{3R(t_\mathrm{o})}}{\sqrt{a_2}\left(\sqrt{a_1 a_2} + 12\kappa\rho(t_\mathrm{o})R(t_\mathrm{o})\right)^2}. \tag{30}$$

Therefore, substituting equations (24) and (30) into equation (29), we obtain

$$n(z) = \frac{48\pi N R(t_\mathrm{o})(\beta c^2 \alpha \rho(t_\mathrm{o}))^2 \sqrt{3R(t_\mathrm{o})}[\sqrt{a_2}-\sqrt{a_1}]^2}{[1+\kappa(\frac{\sqrt{a_2}-\sqrt{a_1}}{\sqrt{a_1 a_2}+12\kappa\rho(t_\mathrm{o})R(t_\mathrm{o})})^2]^3[\sqrt{a_1 a_2}+12\kappa\rho(t_\mathrm{o})R(t_\mathrm{o})]^4}. \tag{31}$$

This equation relates how the number density of galaxies evolves with redshift. Together with equation (28), they constitute our important result in this paper. These results are more general than the results obtained using Einstein field equations of GR without the effects of dark energy (Wamalwa 2016).

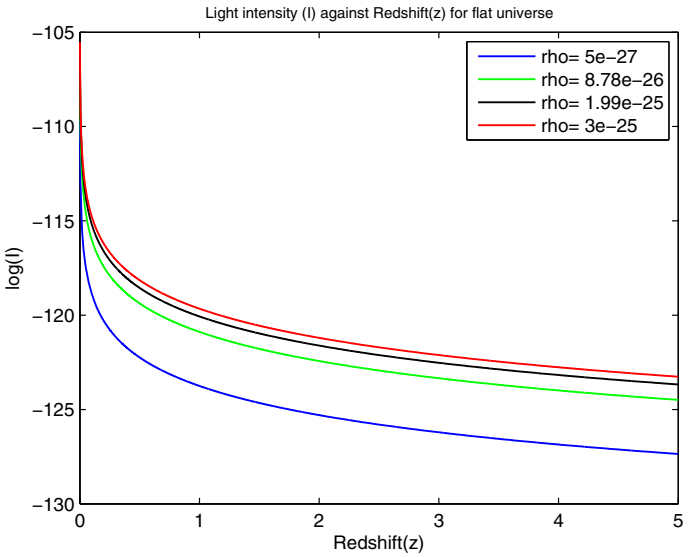

Figure 3. Plot of $\log(I)$ against z for $0 \leq z \leq 5$ and $\kappa = 0$ without cosmological constant (λ).

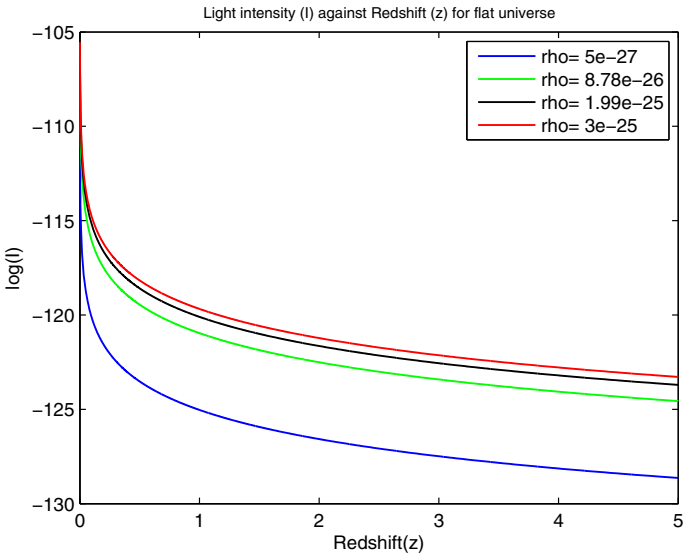

Figure 4. Plot of $\log(I)$ against z for $0 \leq z \leq 5$ and $\kappa = 0$ with cosmological constant (λ).

5. Graphical results

In the last section, we established analytically the relationship between number density of galaxies, redshift and light intensity. Let us now consider the graphical evaluation of our results by writing and running simple computer matlab programs and plotting the results for light intensity-redshift and number density-redshift relations based on equations (28) and (31) for our analysis. In our matlab program, we have used the values of redshift from $z = 0$ to $z = 5$. These redshift values are in line with available statistics. Density of the universe used varies from $\rho(t_o) = 3e^{-25}\,\mathrm{kg\,m^{-3}}$ to $\rho(t_o) = 5e^{-27}\,\mathrm{kg\,m^{-3}}$ while the speed of light used in the program is $c = 3 \times 10^8\,\mathrm{m/s}$. The cosmic scale factor used is $R(t_o) = 9e^{25}\,\mathrm{m}$ (but can be varied appropriately too) and the gravitational constant $G = 6.67 \times 10^{-11}\,\mathrm{m^3\,kg^{-1}\,s^{-2}}$. The curvature of the universe $\kappa = -1, 0, 1$ and the cosmological constant $\lambda = 1.19e^{-52}\,\mathrm{m^{-2}}$. Furthermore, for better results, we have taken logarithm of values of light intensity and number density. Since we are interested in the choice of parameters $\rho(t_o)$ and $R(t_o)$ that would give us the shape of the curve that would fit the experimental result (using unlimited observational data that does not have assumptions about the background geometry), we can assign the number N of galaxies per unit volume of our metric and the constant absolute power L of a galaxy

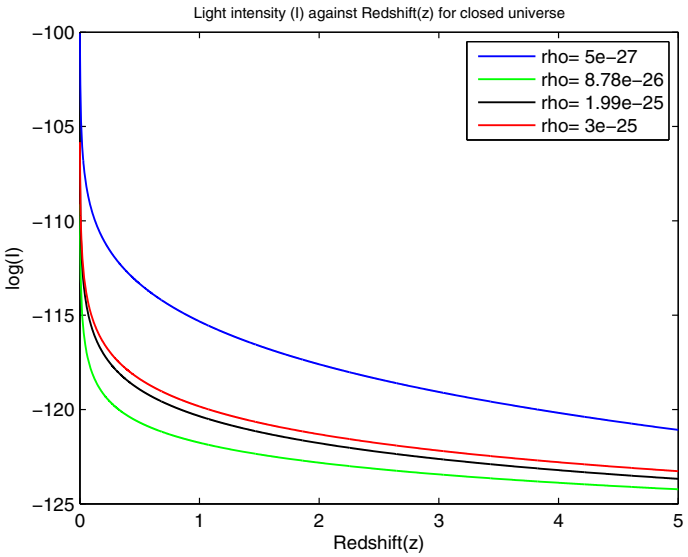

Figure 5. Plot of $\log(I)$ against z for $0 \leq z \leq 5$ and $\kappa = 1$ without cosmological constant (λ).

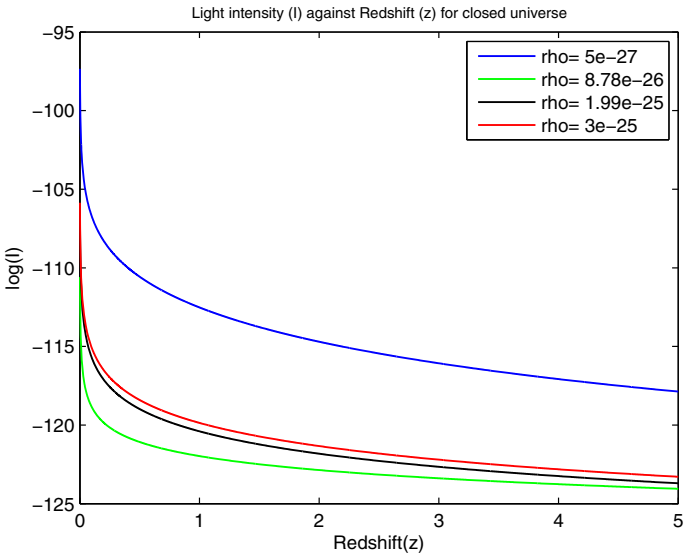

Figure 6. Plot of $\log(I)$ against z for $0 \leq z \leq 5$ and $\kappa = 1$ with cosmological constant (λ).

or star, the arbitrary value 1. If we run our program based on equation (28) for various values of $\rho(t_o)$ and κ (for $R(t_o) = 9e^{25}$m), we obtain the following results (Figures 1–6) for light intensity:

From Fig. 1 to Fig. 6, we observe that light intensity generally decreases with redshift in accordance with our classical expectation. As redshift increases, the ionizing sources decrease because structure formation becomes less advanced. The case of positive curvature describes the closed universe, whose three dimensional space is anologous to the surface of a sphere. As the coordinate of a sphere ranges from zero to one, the r-sphere sweeps out the entire universe leaving it unbounded. We also see that the light curves tend to ultimately converge for this case. The converse is visible for open universe where the light curves tend to ultimately diverge. The light curves for flat universe neither converge nor diverge. These effects are clear when the value of (z) is increased in the program. From our results, it is also clear that light curves are affected by dark energy, density and curvature of the universe e.g., light curves corresponding to density of $5e^{-27}\text{kg/m}^3$ decrease faster in a flat and open universe than in a closed universe. This effect is more pronounced in a flat and open universe driven by dark energy effects, as seen from figures 1 to 4, than one without dark energy.

Let us now look at the graphical results of the evolution of the number density of galaxies n with redshift z

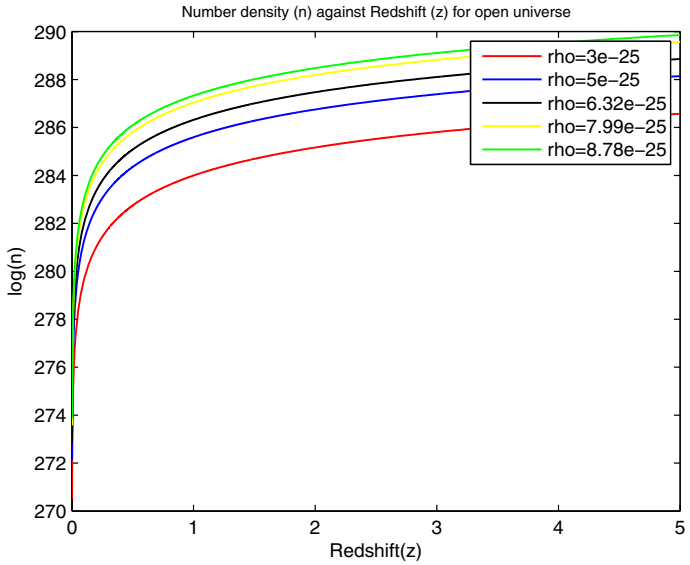

Figure 7. Plot of $\log(n)$ against z for $0 \leq z \leq 5$ and $\kappa = -1$ without cosmological constant (λ).

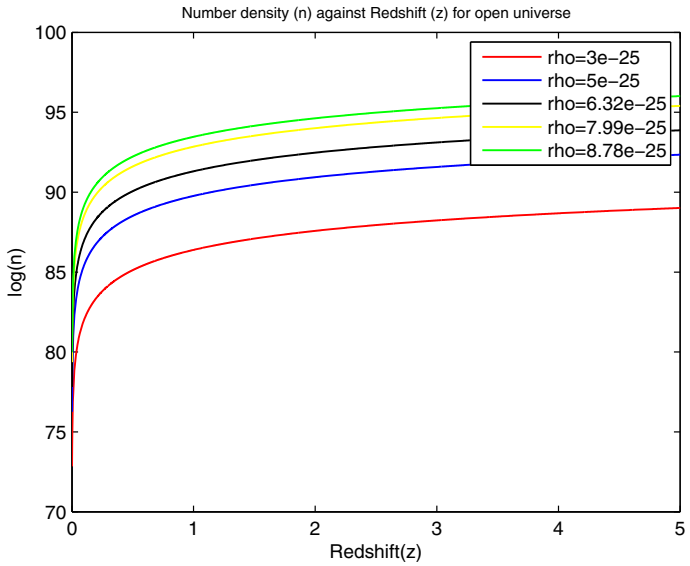

Figure 8. Plot of $\log(n)$ against z for $0 \leq z \leq 5$ and $\kappa = -1$ with cosmological constant (λ).

as given in equation (31). Plots for the number density of galaxies as shown from Figures 7 to 12 reveal that galaxies seem to have formed at a faster rate at the beginning of the universe than at much later time. Structure formation seem to have grown at a fast rate from $z = 0$ until $z \approx 1$ when it started to slow down. However, the rate of structure or galaxy formation seems to be more for a universe without dark energy as compared to one with dark energy. This may be due to continued accelerated expansion of the universe caused by dark energy. The overall expansion of the universe reduces structure formation exponential law and hence inhibits structure formation. For plots of κ that give almost similar curves, the universe may probably be unstable for those values of densities and cosmic scale factor although appropriate scaling can help in differentiating them.

5.1 *How to compare our theoretical and experimental results?*

We have already obtained our graphical results for both light intensity and number density as shown above. Suppose we have accurate observational data (huge enough data and free from errors associated with cosmic distance measurements) measured for redshift, number density and light intensity, then we can compare the

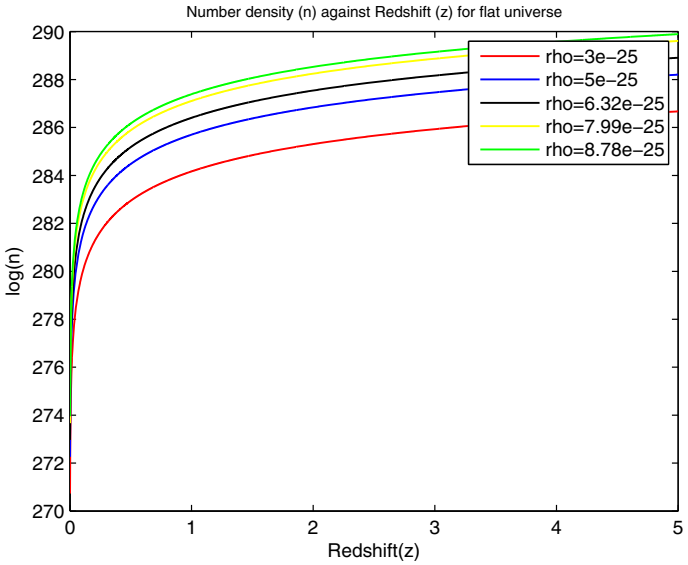

Figure 9. Plot of $\log(n)$ against z for $0 \leq z \leq 5$ and $\kappa = 0$ without cosmological constant (λ).

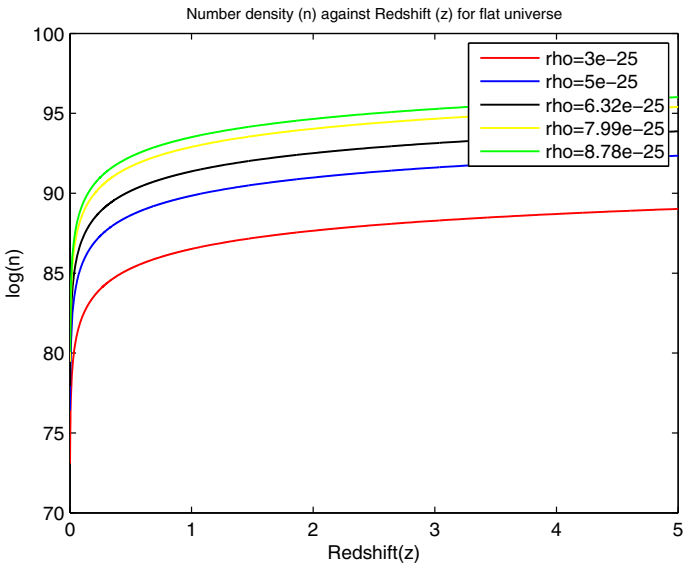

Figure 10. Plot of $\log(n)$ against z for $0 \leq z \leq 5$ and $\kappa = 0$ with cosmological constant (λ).

experimental curve with our theoretical curve by plotting them on the same scale. In this way, we can judge which experimental curve matches our theoretical curve for both light intensity and number density. It is possible that the experimental curve may not fit any of our theoretical curves but lie in between two theoretical curves. If this is the case, then one can choose a new value, say $R(t_o)$, that lies in between the two values of the theoretical curves sandwiching the experimental curve and use it in the corresponding program of light intensity or number density. The process can be repeated until we get a perfect theoretical curve that fits the experimental curve. At this point, we can regard the parameter values $R(t_o)$, $\rho(t_o)$ and κ as the cosmic scale factor, density and curvature of the universe, i.e., flat, open or closed respectively. However, if we cannot get any experimental curve that fits our theoretical curve no matter what the choice of paramters are, then we can disregard the Friedmann model in favour of other models like the fractal model.

6. Summary and conclusions

For a long time, scientists have successfully described structure formation in the universe based on the standard model. However, current tridimensional maps of the universe cast doubt on the validity of this model, in favour of the fractal model, as galaxy redshift surveys probe deeper into the universe uncovering more

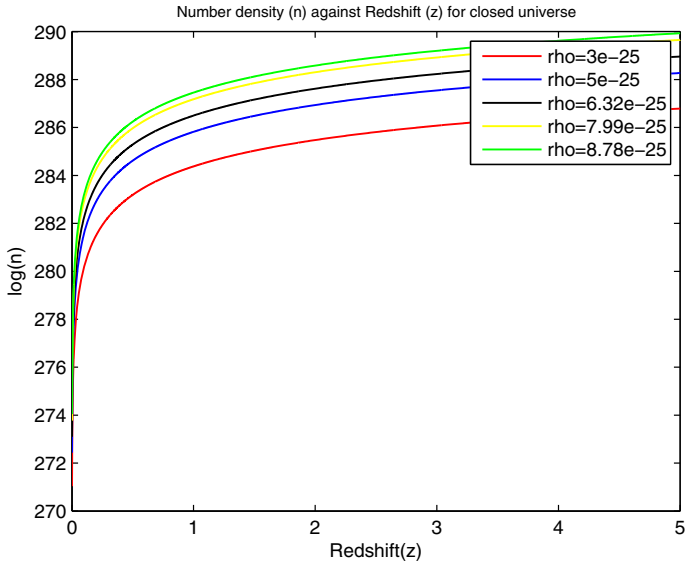

Figure 11. Plot of $\log(n)$ against z for $0 \leq z \leq 5$ and $\kappa = 1$ without cosmological constant (λ).

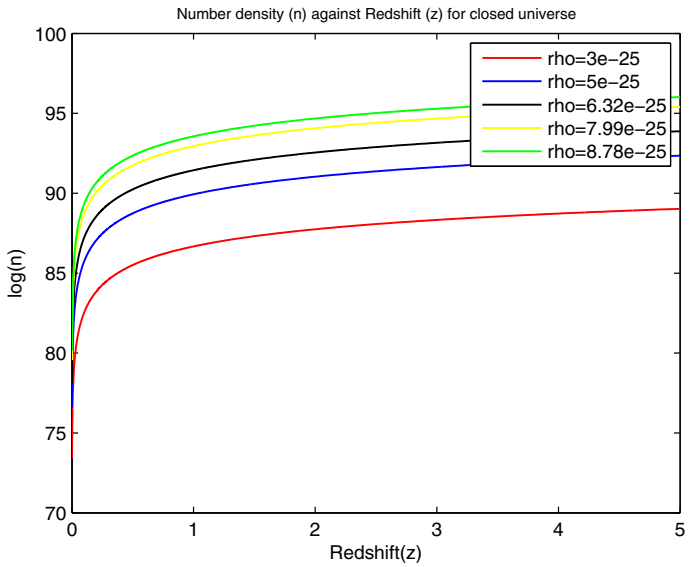

Figure 12. Plot of $\log(n)$ against z for $0 \leq z \leq 5$ and $\kappa = 1$ with cosmological constant (λ).

inhomogeneous structures on large scales. These maps depend on our ability to measure cosmic distance which is associated with lots of errors. Furthermore, the limited available observational data may not be relied upon for accurate results. In this work, we have derived Einstein field equations for a matter-dominated Friedmann universe while considering the effects of dark energy. Analytical and computational results for the evolution of light intensity and number density of galaxies with redshift have been obtained in a suitable form for comparison with future observed dependencies. From our results, light intensity from astronomical objects falls off with redshift and hence, by Hubble law, distance. This is in agreement with the classical results. Thus, the laws of classical physics holds true for open, closed and flat universe. From our number density-redshift relation, there was increased activity of galaxy or structure formation at the beginning of the universe than at later times for open, closed and flat universe. This activity seems to have slowed down at around $z \approx 1$ but structure growth is less pronounced for a universe driven with dark energy than one without. This may be due to the continued accelerated expansion of the universe caused by dark energy that inhibits structure growth. This structure formation rate is in accordance with astrophysical observations and structure formation theory of the standard model. We, therefore, hold a view that the Friedmann model adopted in this work

is correct. Nevertheless, we have prepared our results for experimental test based on future accurate observational data. Subject to availability of this data, we hope, this rests the fractal debate on whether or not the matter-dominated Friedmann universe is homogeneous on large scales.

Acknowledgements

We would like to thank the University of Nairobi for material support of this research work.

References

Borgani, S. 1995, *Phys. Rep.*, **251**, 12, https://doi.org/10.1016/0370-1573(94)00073-C.

Filippenko, A. V. 1998, *Phys. Rep.,* **307**, 14, https://doi.org/10.1016/S0370-1573(98)00052-0.

Joyce, M., Labini, S. F., Gabrielli, A., Montuori, M., Pietronero, L. 2005, *A&A,* **443**, 1, https://doi.org/10.1051/0004-6361:20053658.

Kazuhiro, Y. 2003, *MNRAS,* **341**, 4, https://doi.org/10.1046/j.1365-8711.2003.06477.x.

Labini, F. S., Pietronero, L. 1996, *Astrophys. J.,* **469**, 26, https://doi.org/10.1086/177754.

Michal, B. H. 1989, *Principles of Cosmology and Gravitation*, Institute of Physics Publishing, England, pp. 3–17.

Mureika, J. R. 2007, *JCAP*, **2007**, 05, https://doi.org/10.1088/1475-7516/2007/05/021.

Sarkar, S., Pandey, B. 2016, *MNRASL,* **463**, 1, L12, https://doi.org/10.1093/mnrasl/slw145.

Wamalwa, D. S. 2016, *Int. J. Pure Appl. Math.,* **107**, 4, https://doi.org/10.1051/0004-6361:20053658.